EPR Studies of the Electronic Structure and Dynamic Jahn-Teller Effect in Iron(I) Sandwich Compounds

M. V. Rajasekharan,[1a] S. Giezynski,[1a,b] J. H. Ammeter,*[1a] N. Oswald,[1a] P. Michaud,[1c] J. R. Hamon,[1c] and D. Astruc[1c]

Contribution from the Institute of Inorganic Chemistry, University of Zürich, 8057 Zürich, Switzerland, and Laboratoire de Chimie des Organométalliques, Université de Rennes, 35042 Rennes Cedex, France. *Received March 13, 1981*

Abstract: Variable-temperature (4-300 K) EPR results are reported for the 19-electron sandwich complexes $[\eta^5\text{-}C_5H_5]Fe[\eta^6\text{-}C_6H_6]$ = Fe(Cp,Bz) and $[\eta^6\text{-}C_6(CH_3)_6]_2Fe^+PF_6^-$ = $Fe(hmBz)_2PF_6$ and some ring-alkylated derivatives of the former in the pure form as well as in the dilute form in several diamagnetic host compounds and frozen solutions. The results are consistent with a d^7 configuration for iron, with the unpaired electron in a mainly metal-centered (d_{xz}, d_{yz}) molecular orbital. The variation of the g values in the series and their host lattice dependence are analyzed and explained on the basis of dynamic Jahn-Teller coupling in the effective $^2\pi$ ground state and rhombic splitting caused by the unsymmetrical ligands and/or host lattice potential. The Jahn-Teller coupling strength, k_{JT}, is of the order of unity in these systems, which means that the Jahn-Teller stabilization energy and the effective frequency of the vibronic coupling mode are of comparable magnitude. The Jahn-Teller effect is therefore completely dynamic even at the lowest temperature as has been previously observed also in the case of d^7 metallocenes. The variation of the vibronic overlap integral and k_{JT} with the rhombic distortion is evaluated and discussed. In the case of Fe(Cp,Bz), the variation of polycrystalline line width with temperature is fitted to an Orbach-type formula in order to derive information on the energy of the first excited Kramers' doublet.

Paramagnetic sandwich compounds have been the subject of many EPR investigations in recent years.[2] Besides giving valuable information on the electronic energy level ordering and covalency in the highest occupied molecular orbital, these systems also provide examples of degenerate or nearly degenerate electronic ground states ideally suited for investigations of the Jahn-Teller effect. While some understanding has been achieved for the d^5 and and d^7 metallocenes $Mn(Cp)_2$, $Fe(Cp)_2^+$, $Co(Cp)_2$, and $Ni(Cp)_2^+$ and their ring-substituted derivatives,[5] there is a paucity of data on iron(I) d^7 compounds and also bis(arene) and mixed sandwich systems. Brintzinger et al.[3] have reported the EPR spectrum of a frozen solution of bis(hexamethylbenzene)iron(I) cation in the temperature range 25-80 K and concluded from the observation of an orthorhombic **g** tensor that the system is exhibiting a static Jahn-Teller distortion at 25 K and that the distortion is completely dynamic at 80 K, above which the EPR signal is virtually unobservable. On the basis of our earlier results on orbitally degenerate metallocenes, we favor a somewhat different interpretation: the investigated iron(I) sandwich compound is dynamically distorted at all temperatures, the low symmetry of the observed **g** tensor being due to the asymmetric molecular environment in the solvent cage.[2,4] Iron(I) mixed sandwich systems were also investigated by EPR by Nesmeyanov et al.[5] They have obtained the iron(I) complexes by reduction of the corresponding iron(II) salts and measured the EPR spectrum in frozen dimethoxyethane (DME) solutions. In the case of (η^5-cyclopentadienyl)(η^6-benzene)iron, their assignment[5a] of the $g_\parallel$ and $g_\perp$ values are in reverse order to that of ours, and they have used a wrong sign for the spin-orbit coupling parameter in the interpretation of the g values.[5b] Moreover, the g values reported by them for the other cyclopentadienyl(arene)iron complexes ($g_\parallel$ = 2.07-2.25, $g_\perp$ = 2.006) seem to indicate that they originate from an iron(III) d^5 species rather than a d^7 sandwich compound. In order to characterize more clearly the nature of the vibronic ground state of iron(I) sandwich complexes with respect to both covalency and dynamic Jahn-Teller coupling, we report here detailed low-temperature EPR results for $[\eta^6\text{-}C_6(CH_3)_6]_2Fe^+$, $[\eta^5\text{-}C_5H_5]Fe[\eta^6\text{-}C_6H_6]$, $[\eta^5\text{-}C_5H_5]Fe[\eta^6\text{-}C_6(CH_3)_6]$, $[\eta^5\text{-}C_5(CH_3)_5]Fe[\eta^6\text{-}C_6(CH_3)_6]$, $[\eta^5\text{-}C_5H_5]Fe[\eta^6\text{-}C_6(C_2H_5)_6]$, and $[\eta^5\text{-}C_5H_5]Fe[\eta^6\text{-}C_6(CH_3)_5(C_2H_5)]$, abbreviated as $Fe(hmBz)_2^+$, Fe(Cp,Bz), Fe(Cp,hmBz), Fe(pmCp,hmBz), Fe(Cp,heBz), and Fe(Cp,(pm,et)Bz), respectively, in a number of diamagnetic host systems (Chart I).

Chart I

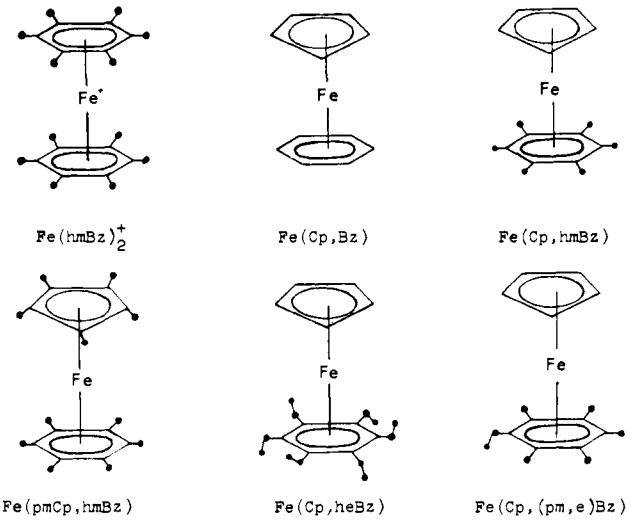

Experimental Section

The synthesis of iron(I) mixed sandwich compounds is discussed elsewhere.[6] The procedure followed for the preparation of $Fe(hmBz)_2PF_6$ was essentially the same as that reported by Fischer and Röhrscheid[7] except for our use of Na/Hg as the reducing agent. The

(1) (a) University of Zürich. (b) Institute of Organic Chemistry and Technology, Technical University (Plitechnica) ul. Koszyowa 7500-662, Warsaw, Poland. (c) Université de Rennes.

(2) Ammeter, J. H. *J. Magn. Reson.* **1978**, *30*, 299-325 and references therein.

(3) Brintzinger, H.; Palmer, G.; Sands, R. H. *J. Am. Chem. Soc.* **1966**, *88*, 623.

(4) (a) Ammeter, J. H.; Zoller, L.; Bachmann, J.; Baltzer, Ph.; Gamp, E.; Bucher, R.; Deiss, E. *Helv. Chim. Acta* **1981**, *64*, 1063-1082. (b) Ammeter, J. H. *Nouv. J. Chim.* **1980**, *4*, 631-637.

(5) (a) Nesmeyanov, A. N.; Solodovnikov, S. P.; Vol'kenau, N. A.; Kotova, L. S.; Sinitsyna, N. A. *J. Organomet. Chem.* **1978**, *148*, C5-C8. (b) Solodovnikov, S. P.; Nesmeyanov, A. N.; Vol'kenau, N. A.; Sinitsyna, N. A.; Kotova, L. S. *Ibid.* **1979**, *182*, 239-243.

(6) Astruc, D.; Hamon, J.-R.; Michaud, P. *J. Am. Chem. Soc.* **1981**, *103*, 758-766.

(7) Fischer, E. O.; Röhrscheid, F. *Z. Naturforsch. B: Anorg. Chem., Org. Chem.* **1962**, *17B*, 483.

0002-7863/82/1504-2400$01.25/0

Table I. EPR Parameters of Fe(I) Sandwich Compounds in Various Host Systems

compd	no.	matrix	g_x	g_y	g_z	$g_\perp$[a]	$g_y - g_x$	"g_{iso}"[b]	tan α	$2\delta_0$[c]	$k_\parallel V$[d]	$X \times 10^2$
Fe(Cp,Bz)	1	isooctane-I[e]	1.295	1.368	1.642	1.331	0.07	1.435	0.852	0.256	0.237	1.0
	2	isooctane-II[e]	1.770	1.838	1.711	1.804	0.068	1.773	1.850	0.555	0.306	0.96
	3	$Fe(Cp)_2$-III	1.881	1.944	1.746	1.912	0.063	1.857	2.62	0.79	0.359	0.90
	4	$Fe(Cp)_2$-IV	1.881	1.944	1.721	1.912	0.063	1.849	2.62	0.79	0.395	0.89
	5	*n*-pentane	1.896	1.962	1.789	1.929	0.066	1.882	2.77	0.83	0.314	0.98
	6	$Fe(Cp)_2$-II	1.911	1.976	1.759	1.943	0.065	1.882	2.99	0.90	0.383	0.94
	7	$Fe(MeCp)_2$[f]	1.916	1.980	1.761	1.948	0.064	1.886	3.06	0.92	0.388	0.93
	8	$Ru(Cp)_2$	1.917	1.983	1.757	1.950	0.066	1.886	3.07	0.92	0.396	0.97
	9	$Fe(Cp)_2$-I	1.923	1.987	1.768	1.955	0.064	1.893	3.18	0.95	0.390	0.95
Fe(Cp,hmBz)	10	oxn prod[g]	1.984	2.052	1.841	2.018	0.068	1.959	5.3	1.6	0.43	1.03
	11	DME[h]	2.000	2.063	1.864	2.032	0.063	1.976	7.2	2.2	0.50	0.97
	12	pure						1.97				
$Fe(hmBz)_2^+$	13	$Re(hmBz)_2PF_6$	1.994	2.088	1.868	2.041	0.094	1.983	5.5	1.6	0.37	1.45
	14	ethanol-water	1.996[i]	2.086[i]	1.865[i]	2.041	0.090	1.982	5.7	1.7	0.40	1.39
	15	$Fe(Cp,hmBz)PF_6$[j]	1.998	2.084	1.865	2.041	0.086	1.982	6.1	1.8	0.43	1.31
	16	pure	2.01	2.08	1.861	2.05	0.07	1.98	8	2.5	0.6	1.17
Fe(pmCp,hmBz)	17	DME[h]	2.002	2.062	1.912	2.032	0.060	1.992	7.5	2.3	0.34	0.95
	18	pure						1.96				
Fe(Cp,heBz)	19	DME[h]	2.003	2.059	1.896	2.031	0.056	1.986	8	2.4	0.44	0.88
	20	pure[k]	1.908	1.995	1.849	1.951	0.087	1.92	2.8	0.8	0.23	1.33
Fe(Cp,(pm,e)Bz)	21	DME[h]	2.006	2.053	1.850	2.029	0.047	1.970	>10	3.2	~0.8	0.72

[a] $g_\perp = (g_x + g_y)/2$. [b] "g_{iso}" $= (g_x + g_y + g_z)/3$. [c] $\times 10^3$ cm^{-1}; $2\delta_0 = \zeta \tan \alpha$, with $\zeta = 0.300 \times 10^3$ cm^{-1} (see note 16). [d] For $k_\parallel = 0.85$ (see note 18). [e] The isooctane matrix provided the two most axial sites observed in this series of compounds. [f] Bis(methylcyclopentadienyl)iron(II). [g] This is a partially air-oxidized (to the extent of 95%) sample of Fe(Cp,hmBz); the oxidation product is $Fe[Cp,\eta^5\text{-}C_6(CH_3)_5CH_2]$. [h] 1,2-Dimethoxyethane. [i] Reference 3. [j] Nesmeyanov, A. N.; Vol'kenau, N. A.; Bolesova, I. N. *Dokl. Akad. Nauk SSSR* 1963, *149*, 615–618, *Ibid.* 1966, *166*, 607–610. [k] An additional broad line ($g \sim 2$) is observed in this case (see Figure 5); therefore the assignment of the g values is in doubt, and the parameters derived are likely to be in error.

diamagnetic compounds used for doping were either purchased or prepared by previously reported procedures, literature references to which are included in Table I. Dilute samples for EPR measurements were prepared by dissolving the host compound and 0.5–1% of the paramagnetic compound in 1,2-dimethoxyethane (DME) and evaporating the solution to dryness. $Fe(hmBz)_2$ doped in the corresponding rhenium salt was obtained by reprecipitation from an acetone solution using diethyl ether. Due to the extreme air sensitivity of these compounds, all preparations were carried out in an atmosphere of pure dry nitrogen. The unsubstituted mixed sandwich, Fe(Cp,Bz), is also thermally unstable above −20 °C, and hence in the present study solutions containing this compound were directly used for doping in the diamagnetic host systems. EPR tubes were charged in a nitrogen-filled glovebox and sealed under vacuum. All EPR spectra were measured with a Varian X-band spectrometer fitted with an Oxford liquid helium cryostat and variable-temperature equipment. The magnetic field was calibrated with an NMR gaussmeter and the microwave frequency was measured with a frequency counter. Spectra were measured from 4 K upwards till the signals were broadened beyond detection (~80 K in all cases).

In the case of Fe(Cp,Bz) diluted in $Fe(Cp)_2$, where four chemically inequivalent sites were observed, the powder spectrum was fitted by using a locally written simulation program in order to obtain accurate g values. In all other cases the three principal g values were measured directly from the polycrystalline or frozen glass spectra.

Theory

As in metallocenes, the d-orbital splitting in bis(arene) and mixed sandwich molecules can be described by a pseudoaxial symmetry[8] even though the exact molecular point groups are D_{6h} (bis(arene)) and C_s (mixed sandwiches). Both our own semiempirical molecular orbital calculations of the extended Hückel type[9] and the INDO calculations of Clack and Warren[8b,10] indicate that the low symmetry splittings in the degenerate molecular orbitals of Fe(Cp,Bz) are negligible. Thus, analogous to $Co(Cp)_2$, the ground state is expected to be $^2E_{1g}$ (D_{6h} notation) or $^2\pi$ ($C_{\infty v}$ notation), with the unpaired electron in the e_{1g} orbital having mainly (d_{xz}, d_{yz}) character. All our EPR spectra can be interpreted with this ground state even though the INDO results[10] favor the unpaired electron on a ligand molecular orbital in the case of mixed sandwich molecules. In addition, the Mössbauer isomer shifts and quadrupole splittings (IS = 0.73–0.75 mm s^{-1} with respect to metallic iron, QS = 1.5 mm s^{-1} at 4.2 K)[6,11] and the proton chemical shifts[6,13] are also consistent with a d^7 configuration. Spin–orbit coupling and the orthorhombic potential of the host lattice in combination with vibronic coupling will tend to lift this degeneracy. If one takes into account all these interactions, the total molecular Hamiltonian can be written as

$$\mathcal{H} = \mathcal{H}_{axial}(q) + \mathcal{H}_{rhombic}(q) + \mathcal{H}_{spin\text{-}orbit}(q) + \mathcal{H}_{nucl}(Q) + \mathcal{H}'(q,Q) \quad (1)$$

where q and Q refer to electronic and nuclear coordinates, respectively. If the vibronic coupling term $\mathcal{H}'$ (being responsible for a dynamic Jahn–Teller effect even at 0 K) is not taken into account, the eigenfunctions of the above Hamiltonian can be approximated as single Born–Oppenheimer products; thus for the ground Kramers' doublet we have

$$\Psi^\pm = \{c|xz\rangle^\pm \mp is|yz\rangle^\pm\}\chi \quad (2)$$

where $c^2 = {}^1/_2 + {}^1/_2\{1 + (\zeta/2\delta)^2\}^{-1/2}$ and $c^2 + s^2 = 1$.[14,15] $|xz\rangle$ and $|yz\rangle$ are molecular orbitals, χ is a vibrational wave function, ζ is the effective one-electron spin–orbit coupling constant[16]

(8) (a) Warren, K. D. *Struct. Bonding (Berlin)* **1976**, *27*, 45–159. (b) Clack, D. W.; Warren, K. D. *Ibid.* **1980**, *39*, 1–41.

(9) Rajasekharan, M. V.; Giezynski, S.; Astruc, D.; Ammeter, J. H. "Proceedings of the Twenty-First International Conference on Coordination Chemistry"; Toulouse, 1980; p 393.

(10) Clack, D. W.; Warren, K. D. *J. Organomet. Chem.* **1978**, *152*, C60–C62.

(11) An interesting temperature dependence has been observed for the quadrupole splitting. In all the Fe(I) sandwich compounds investigated, the QS varies from ~1.5 to 0.5 mm s^{-1} as the temperature is raised from 4.2 to 300 K, with no change in isomer shift. In the case of Fe(Cp,hmBz), Fe(Cp,heBz), and Fe(Cp,(pm,e)Bz), an additional doublet with the same chemical shift is observed in a certain temperature range. It is not clear at present whether these effects are due to thermal population of excited states, phase transitions, anisotropic relaxation via molecular motion (proposed by Fitzsimmons[12] in the case of diamagnetic mixed sandwich cations), or to a combination of these mechanisms. The possibility of low-spin–high-spin equilibrium can be ruled out because there is no evidence for it in the EPR spectra of pure samples or from preliminary magnetic susceptibility measurements (4–300 K) on Fe(Cp,hmBz). A clue to the interpretation will hopefully be obtained from Mössbauer measurements in dilute samples.

(12) Fitzsimmons, B. W. *J. Phys., Colloq. (Orsay, Fr.)* **1980**, *41*, 33–37.

(13) Cozak, D. "Proceedings of the Twenty-First International Conference on Coordination Chemistry"; Toulouse, 1980; p 390, and personal communication.

(14) (a) Maki, A. H.; Berry, T. E. *J. Am. Chem. Soc.* **1965**, *87*, 4437–4447. (b) Nussbaum, M.; Voitländer, H. *Z. Naturforsch. A* **1965**, *20A*, 1417–1424. (c) Prins, R. *Mol. Phys.* **1970**, *19*, 603–620.

(15) Ammeter, J. H.; Swalen, S. D. *J. Chem. Phys.* **1972**, *57*, 678–698.

(always positive), and 2δ is the rhombic splitting. The last term in eq 1 produces a vibronic mixing of ground and excited Kramers' doublets so that the ground-state wave function is modified as

$$\Psi^{\pm} = c|xz\rangle^{\pm}\chi_1 \mp is|yz\rangle^{\pm}\chi_2 \quad (3)$$

The vibrational functions χ_1 and χ_2 are different but not orthogonal. The spin–orbit coupling will also produce a mixing of the higher excited states with the ground state. Including only the doublet states (σ and δ) to first order in perturbation theory, one finally obtains the ground-state wave function as follows:

$$\Psi^{\pm} = c|xz\rangle^{\pm}\chi_1 \mp is|yz\rangle^{\pm}\chi_2 \mp (3^{1/2}/2)(c'\chi_1 + s'\chi_2)|z^2\rangle^{\mp}X_1' \pm (1/2)(c'\chi_1 - s'\chi_2)|x^2 - y^2\rangle^{\mp}X_2' + (1/2)i(c'\chi_1 - s'\chi_2)|xy\rangle^{\mp}X_3' \quad (4)$$

where $X_i' = -(c_i/c_\pi)(\zeta/\Delta E_i)$, with c_π and c_i ($i = \sigma, \delta$) being the metal 3d coefficients in the molecular orbital describing the ground and excited states, respectively. It is reasonable[17] to use the average energy approximation and to represent the three excited states by a single parameter. One then obtains the following expressions for the elements of the **g** tensor, where $g = 2.0023$ is the free electron g value:

	Vibronic coupling case	Static limit (first order in ζ)
g_z	$g_e - 2k_\parallel V\cos\alpha$	$g_e - k_\parallel\zeta/\delta$
$g_\perp = (g_x + g_y)/2$	$(g_e + 5X)\sin\alpha$	$g_e + 5X$
$\delta g = g_y - g_x$	$6(1 + V\cos\alpha)X$	$6X$

(5)

In the above equations, V is the vibrational overlap integral, $\langle\chi_1|\chi_2\rangle$, $\tan\alpha = (c'^2 - s'^2)/2c's'$, and $k_\parallel$ is an orbital angular momentum reduction factor.[18] X is given by $k_\perp\zeta/\overline{\Delta E}$, where $k_\perp$ is again a reduction factor[18] due to covalency and overlap terms and $\overline{\Delta E}$ is the average of the three excitation energies. In the static limit, $V = 1$ and $\tan\alpha$ is simply the ratio of the orthorhombic splitting to the effective spin–orbit coupling parameter ($2\delta/\zeta$). In the dynamic coupling case, which results whenever the static splitting is less than or of the same order of magnitude as one vibrational quantum, only the ratio $\tan\alpha$ and not δ can be directly determined from the EPR data. However, as the static splitting increases, $\tan\alpha$ will approach infinity and at sufficiently large values of $\tan\alpha$ the static approximation will be adequate for the description of the EPR parameters. It is important to note that the dynamic case corresponds to a delocalization (both in the electronic and in the structural sense) of the system along the approximately circular Jahn–Teller minimum and not to a rapid equilibrium between different discrete static distorted configurations.[2,4,15] This is due to the topology of the $E \otimes e$ type Jahn–Teller potential surface, which allows for a delocalization of the ground vibrational wave function along the circular Jahn–Teller valley.[21] "Warping" terms introducing secondary minima and barriers along the Jahn–Teller valley do not usually have a significant influence on the nature of the vibronic ground state in the case of weak to moderate coupling, i.e., for Jahn–Teller energies smaller or of the same order of magnitude as a vibrational quantum.[21] Furthermore, Engelking and Lineberger[22] have recently shown that second-order terms vanish for symmetry reasons in systems having a fivefold axis of symmetry. Therefore, no significant barriers can be expected in the case of metallocenes. Our EHMO calculations do not produce any barriers for either the $M(Cp)_2$ or $M(Bz)_2$ d^7 case. Experimental evidence for negligible higher order ("warping") effects can also be found in the laser spectroscopy work of Cossart-Magos et al.[23] and Miller et al.[24] on the substituted benzene ring radicals in the gas phase.

It is important to distinguish this dynamic Jahn–Teller motion at absolute zero from additonal dynamic distortions arising upon warming to higher temperatures via thermal population of excited states (in our case the upper Kramers' doublet). No EPR signals attributable to the excited Kramers' doublet have ever been observed. Rapid spin–lattice relaxation broadens the EPR spectrum before the upper level is populated to any significant degree in all cases of orbitally degenerate sandwich compounds encountered so far .[2,4,15] Effects from thermal population of excited electronic levels and ring rotation can however be seen in Mössbauer spectra,

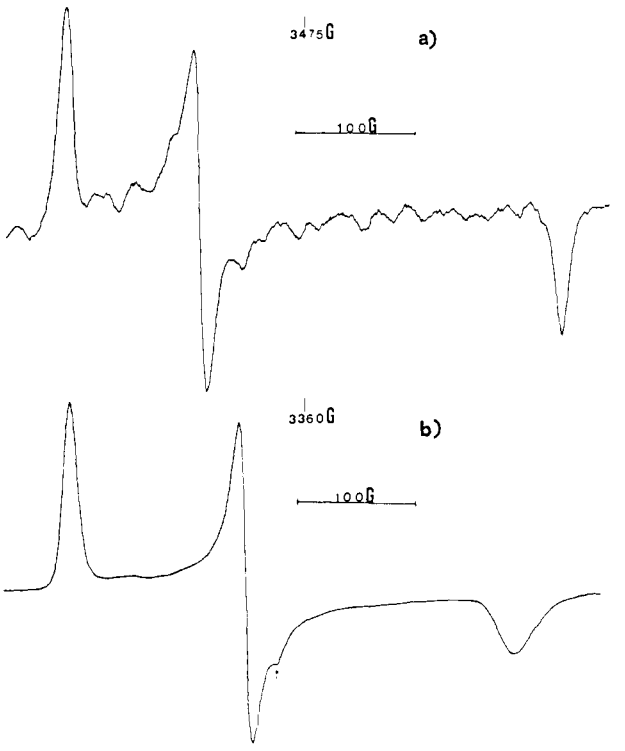

Figure 1. EPR spectra of (a) Fe(Cp,Bz) diluted in polycrystalline $Ru(Cp)_2$ at 4 K (X-band, 9.0868 GHz) and (b) $Fe(hmBz)_2PF_6$ diluted in polycrystalline $Re(hmBz)_2PF_6$ at 5 K (X-band, 9.2441 GHz). The arrow indicates a signal from an unidentified impurity.

(16) The spin–orbit coupling constant is reduced from the free ion value ($\zeta_0 = 357$ cm^{-1} for Fe^+ and 412 cm^{-1} for Fe^{2+}) by the reduction in the effective nuclear charge as well as by covalent delocalization. The effective spin–orbit coupling parameter $\zeta = c_\pi^2\zeta_d$, where c_π is the 3d atomic orbital coefficient in the molecular orbital containing the unpaired electron and $\zeta_d \sim \zeta_0$. With $c_\pi^2 = 0.830$ obtained from EHMO calculations,[18] one gets $\zeta = 296$ cm^{-1}, assuming the free ion value for Fe^+ or 342 cm^{-1} if ones uses the Fe^{2+} value. We have set $\zeta = 300$ cm^{-1} in our calculations.

(17) In the analogous case of cobaltocene, the doublet excited states are clustered around 20×10^3 cm^{-1}.[15]

(18) EHMO calculations were carried out for Fe(Cp,Bz) and $Fe(Bz)_2^+$ by using standard procedures.[19] The following bond lengths were employed: $Fe-C(C_6H_6) = 2.100$ Å, $Fe-C(C_5H_5) = 2.144$ Å (taken from the crystal structure data[34] on Fe(Cp,hmBz)), C–C = 1.423 Å for C_6H_6 and 1.420 Å for C_5H_5, and C–H = 1.1 Å. The basis set for Fe consisted of 3d (double ζ) and 4s (quadruple ζ) functions for the $3d^64s^2$ conflguration (Clementi, E.; Roetti, C. *At. Data Nucl. Data Tables* **1974**, *14*, 433) and 4p functions for the $3d^74p$ configuration (Richardson, J. W.; Powell, R. R.; Nieuwpoort, W. C. *J. Chem. Phys.* **1963**, *38*, 796–801). The orbital angular momentum matrix elements over the molecular orbitals were evaluated by using a previously described computer program.[20] These matrix elements were employed for calculating the reduction factors $k_\parallel$ and $k_\perp$, defined as follows: $k_\parallel = \langle xz|l_z|iyz\rangle$; if $|xz\rangle$ and $|yz\rangle$ are written as $|xz\rangle = c_\pi|3d_{xz}\rangle - c_\pi'|\phi_{\pi(xz)}{}^L\rangle$ and $|yz\rangle = c_\pi|3d_{yz}\rangle - c_\pi'|\phi_{\pi(xz)}{}^L\rangle$, then $k_\parallel = 1 - c_\pi'^2(1 - \gamma_\parallel)$, where $\gamma_\parallel = \langle\phi_{\pi(xz)}{}^L|l_z|i\phi_{\pi(yz)}{}^L\rangle$. $k_\perp{}^\sigma = 1 + (c_\sigma'/c_\pi)S_\pi + (c_\sigma'/c_\sigma)S_\sigma - (c_\pi'c_\sigma'/3^{1/2}c_\pi c_\sigma)\gamma_\perp{}^\sigma$, and $k_\perp{}^\delta = 1 + (c_\pi'/c_\pi)S_\pi + (c_\pi'/c_\pi)S_\pi + (c_\delta'/c_\delta)S_\delta - (c_\pi'c_\delta'/c_\pi c_\delta)\gamma_\perp{}^\delta$, where $\gamma_\perp{}^{\sigma,\sigma} = \langle\phi_\pi{}^L|l_x|\phi_{\sigma,\delta}{}^L\rangle$. The numerical results for Fe(Cp,Bz) and $Fe(Bz)_2^+$ (in parentheses) are as follows: $c_\pi = 0.923$ (0.911), $c_\pi' = 0.562$ (0.583), $S_\pi = -0.161$ (−0.160), $k_\parallel = 0.854$ (0.839), $\gamma_\parallel = 0.538$ (0.526), $k_\perp{}^\sigma = 0.877$ (0.858), $\gamma_\perp{}^\sigma = 0.453$ (0.819), $k_\perp{}^\delta = 0.801$ (0.742), and $\gamma_\perp{}^\delta = 0.469$ (0.536).

(19) Ballhausen, C. J.; Gray, H. B. "Molecular Orbital Theory"; W. A. Benjamin: Reading, MA, 1964. See also: Ammeter, J. H.; Bürgi, H.-B.; Thibeault, J. C.; Hoffman, R. *J. Am. Chem. Soc.* **1978**, *100*, 3686–3692.

(20) Ichimura, H.; Rauk, A. *J. Chem. Phys.* **1973**, *59*, 5720–5724.

(21) (a) Englman, R. "The Jahn–Teller Effect in Molecules and Crystals"; Wiley: New York, 1972. (b) Sturge, M. D. *Solid State Phys.* **1968**, *20*, 91–211. (c) Bersuker, I. B. *Coord. Chem. Rev.* **1975**, *14*, 357–412.

(22) Engelking, P. C.; Lineberger, W. C. *J. Chem. Phys.* **1977**, *67*, 1412–1417.

(23) Cossart-Magos, C.; Cossart, D.; Leach, S. *Chem. Phys.* **1979**, *41*, 345–362.

(24) Sears, T.; Miller, T. A.; Bondybey, V. E. *J. Chem. Phys.* **1980**, *72*, 6070–6080.

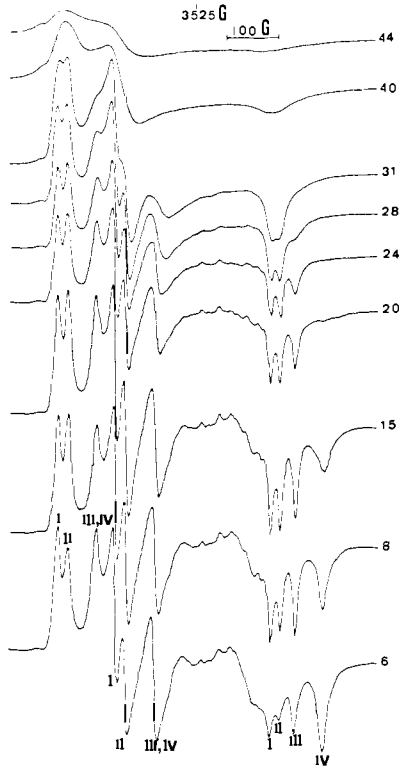

Figure 2. Temperature dependence of the EPR spectrum of Fe(Cp,Bz) diluted in polycrystalline $Fe(Cp)_2$ (X-band, 9.077 GHz). Temperature readings are in kelvin. Spectra at higher temperature are shown on an expanded vertical axis scale.

to be discussed in a future paper.[25]

In the linear coupling approximation involving a single Jahn–Teller-active vibration, it is possible to relate the energy separation between the two lowest Kramers' doublets (ΔE, not to be confused with $\overline{\Delta E}$ defined earlier) with δ and ζ by the following approximate relation due to Ham:[26]

$$\Delta E = (p^2\zeta^2 + 4q^2\delta^2)^{1/2} \quad (6)$$

p and q are the Ham reduction factors for spin–orbit coupling and crystal-field splitting, respectively. In the linear single-mode coupling case, $q = {}^1/_2(1 + p)$. If an independent estimate of ΔE can be obtained, this equation can be used to evaluate the reduction factors and hence the strength of the Jahn–Teller coupling and to verify the validity of the single-mode approximation. ΔE cannot be directly derived from EPR g and A values. The proximity of the upper doublet can however influence the spin-relaxation behavior of the ground level in case an Orbach-type relaxation mechanism[27] prevails. We therefore measured also the temperature dependence of the EPR line width in the accessible range. A more direct access to the ΔE will be through electronic Raman scattering[28] or inelastic neutron scattering[29] experiments. Successful neutron scattering experiments have already been performed for ferrocenium cation,[30] but not yet for the compounds discussed in this paper.

Results

(a) EPR in Dilute Samples. The EPR spectra of Fe(Cp,Bz) doped in $Ru(Cp)_2$ shown in Figure 1a and of $Fe(hmBz)_2^+$ doped in $Re(hmBz)_2PF_6$ shown in Figure 1b are typical for iron(I) sandwich compounds, and they clearly show a nonaxial **g** tensor.

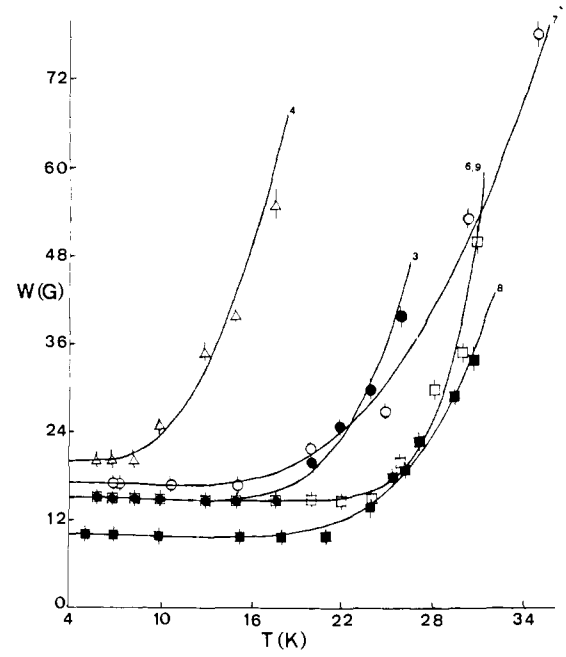

Figure 3. Temperature dependence of the width of the highest field powder line of Fe(Cp,Bz) in various host lattices: (□) $Fe(Cp)_2$-I,II; (●) $Fe(Cp)_2$-III; (△) $Fe(Cp)_2$-IV; (■) $Ru(Cp)_2$; (○) $Fe(MeCp)_2$. The numbers on the curves correspond to Table I.

Figure 2 shows the spectrum of Fe(Cp,Bz) diluted in $Fe(Cp)_2$. Four chemically inequivalent sites are present in this case which we attribute to the slightly different environment of the dopant molecules at four sites in the low-temperature form of ferrocene, which has been investigated by X-ray crystallography[31] and neutron diffraction.[32] Since there are two chemically inequivalent noncentrosymmetric sites for metallocene molecules with two equal hydrocarbon rings,[33] four sites are expected (with possibly different populations) for mixed sandwich compounds with two different ligand rings. The **g** tensors for the individual sites could be assigned by following the temperature variation of the spectrum (Figure 2) and also by computer simulation. The results of the **g** tensor analysis for all the systems investigated are presented in Table I. As the temperature is raised from 4 K, in all cases the signal initially becomes smaller in amplitude without appreciable broadening. At a certain temperature, characteristic for each site, the signal starts broadening rapidly without shifting and becomes virtually undetectable above ~80 K. An attempt was made to fit the temperature-dependent contribution to the line width (W) to an Orbach-type model[27] for spin–lattice relaxation by using the equation

$$W = 1/T_1 = B\Delta E^3 e^{-\Delta E/kT} \quad (7)$$

where ΔE is the energy separation between the two lowest Kramers' doublets and B is related to the inverse lifetime of the excited state. In estimating $1/T_1$, we made the simplifying assumption that the total line width contained a temperature-independent or weakly temperature-dependent contribution and a strongly temperature-dependent contribution arising from the Orbach process. A plot of log W vs. $1/T$ can be used to estimate ΔE. W is the powder line width, which we found to be proportional to the single-crystal width. The proportionality constant was determined in a typical case by computer simulation to be ~1.5 and is essentially temperature independent. However, as seen from eq 7, this constant affects only the intercept of the log W vs. $1/T$ plot and not ΔE, which is obtained from the slope. From Figure 3 it appears that the model is valid in a certain temperature range

(25) Rajasekharan, M. V.; Ammeter, J. .; Michaud, P.; Astruc, D.; Mariot, J. P.; Varret, F., unpublished results.
(26) Ham, F. S. *Phys. Rev.* [*Sect.*] *A* **1965**, *138A*, 1727–1740.
(27) Orbach, R.; Stapleton, H. J. In "Electron Paramagnetic Resonance"; Geschwind, S., Ed.; Plenum Press: New York, 1972; pp 121–216.
(28) Gächter, B. F.; Koningstein, J. A.; Aleksanjan, V. T. *J. Chem. Phys.* **1975**, *62*, 4628–4633.
(29) Furrer, A.; Güdel, H. U. *J. Magn. Magn. Mater.* **1979**, *14*, 256–264.
(30) Ammeter, J. H.; Furrer, A.; Hulliger, J., unpublished results.
(31) Seiler, P.; Dunitz, J. D. *Acta Crystallogr., Sect. B* **1979**, *B35*, 1068–1074.
(32) Takusagawa, F.; Koetzle, T. F. *Acta Crystallogr., Sect. B* **1979**, *B35*, 1074–1081.
(33) Schweiger, A.; Wolf, R.; Günthard, Hs. H.; Ammeter, J. H.; Deiss, E. *Chem. Phys. Lett.* **1980**, *71*, 117–122.

Table II. ΔE Obtained from Experimental Line Width Variation[a] together with the Static Splitting (2δ) and the Jahn-Teller Coupling Constant (k_{JT}) from g Values[b] for Fe(Cp,Bz)

matrix	ΔE, $\times 10^3$ cm^{-1}	2δ, $\times 10^3$ cm^{-1}	k_{JT}
isooctane-I	c	0.30	1.13
isooctane-II	c	0.50	1.10
$Fe(Cp)_2$-IV	0.037 (3)	0.72	0.83
$Fe(MeCp)_2$	0.083 (12)	0.76	0.81
$Fe(Cp)_2$-III	0.117 (10)	0.69	0.89
$Ru(Cp)_2$	0.130 (11)	0.92	0.81
$Fe(Cp)_2$-I	0.251 (25)	0.78	0.81
$Fe(Cp)_2$-II	0.251 (25)	0.76	0.81

[a] Via eq 7; the standard deviations in the least significant figures obtained from the regression analysis are given in parentheses. [b] Obtained by combining V and tan α from the g tensor analysis with the results from the diagonalization of the vibronic Hamiltonian for an assumed frequency of 678 cm^{-1} and spin-orbit coupling parameter of 330 cm^{-1} (see text). [c] No line width fitting was done.

for all the systems for which detailed line width data are available. The ΔE values obtained by this procedure are collected in Table II.

(b) EPR in Pure Solid Samples. EPR measurements were also done on pure polycrystalline samples of Fe(Cp,hmBz), Fe(Cp,heBz), Fe(pmCp,hmBz), and $Fe(hmBz)_2PF_6$. In the case of $Fe(hmBz)_6PF_6$ and Fe(Cp,heBz), the principal g values could be obtained from the spectra. In the other two cases only unresolved lines were obtained. There is evidence for antiferromagnetic exchange interaction in Fe(pmCp,hmBz) and $Fe(hmBz)_2$. In both cases, there is a substantial reduction in the amplitude of the unsaturated EPR signal at low temperatures (<6 K). In the case of Fe(Cp,hmBz), an additional broad line ($\Delta H \sim 2000$ G) is found to appear at 45 K. This line has an effective g value of 3.47 (Figure 4). The relative amplitude and the temperature range in which it is observable seem to vary from one preparation to another. As the sample is warmed this line moves to higher fields and appears considerably narrowed ($\Delta H = 750$ G), with $g = 2.129$ at 300 K. This is the only compound in which an EPR line could be observed above 80 K. A broad signal is also observed superimposed on the main signal in Fe(Cp,heBz) (Figure 5). However, this signal is completely broadened out at 70 K. No explanation is offered at present for the origin and temperature dependence of the broad signals. There could be several possible reasons, viz., temperature-dependent exchange coupling, slow magnetic phase transition, spin equilibrium, or the presence of decomposition or oxidation products. These observations could be of some relevance for the interpretation of the Mössbauer spectra to be reported elsewhere.[25]

Discussion

From eq 5, it is clear that the lowest g value must be assigned to g_z. If one assumes a static distortion, this will lead to a splitting of the e_{1g} level in the range 2400–6600 cm^{-1} for the systems reported here. Such large splittings are not expected from molecular orbital calculations or from the available crystal structure data.[34] This fact coupled with the fast relaxation strongly argues for a vibronic coupling mechanism. In the absence of such a mechanism, one will have to introduce an unreasonably small orbital reduction factor ($k_\parallel$) in order to account for the observed g values. However, one would not expect $k_\parallel$ to vary appreciably for the same compound in different host systems.

A plot of $k_\parallel V$ vs. tan α is given in Figure 6. In the absence of nuclear hyperfine data, it is not possible to evaluate $k_\parallel$ and V separately. We have attempted to rationalize this plot on the basis of possible Jahn–Teller coupling mechanisms. For d^7 metallocenes and bis(benzene) complexes there are three Jahn–Teller-active vibrations, viz., in-plane C–C stretch (r), in-plane C–C–C bending (δ), and out-of-plane torsion (τ) as shown in Figure 7. The

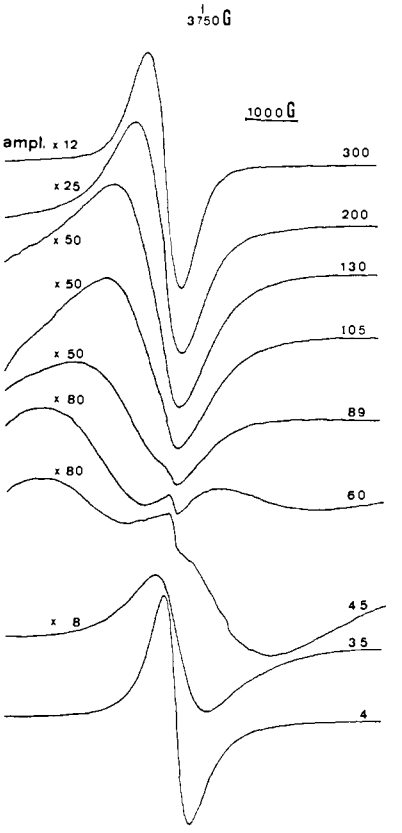

Figure 4. X-band EPR spectra of an undiluted polycrystalline sample of Fe(Cp,hmBz) at various temperatures (K).

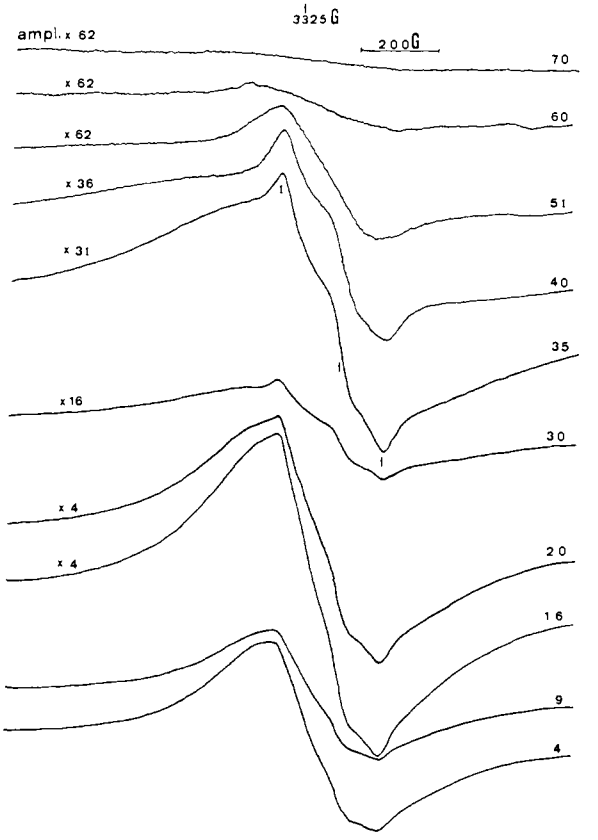

Figure 5. X-band EPR spectra of an undiluted polycrystalline sample of Fe(Cp,heBz) at various temperatures (K). The arrows correspond to the g values reported in Table I.

(34) Astruc, D.; Hamon, J.-R.; Althoff, G.; Roman, E.; Batail, P.; Michaud, P.; Mariot, J.-P.; Varret, F.; Cozak, D. *J. Am. Chem. Soc.* **1979**, *101*, 5445–5447.

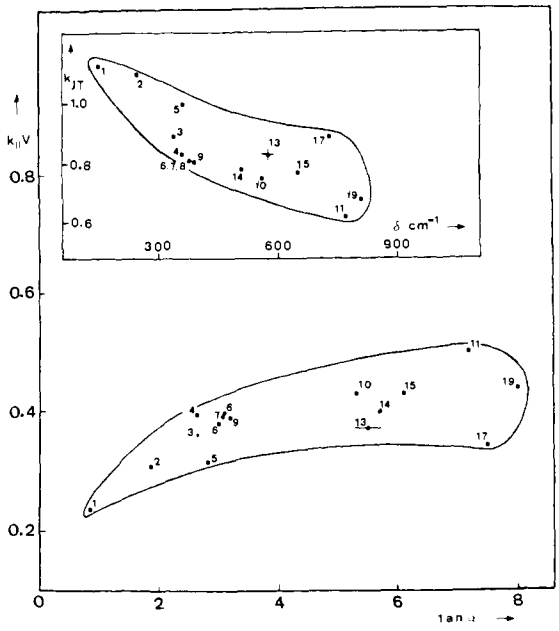

Figure 6. $k_{\parallel}V$ values for Fe(I) sandwich compounds as a function of tan α. Inset: Jahn–Teller coupling constant, k_{JT}, as a function of δ (half the rhombic splitting). Error bars are provided for one representative point, estimated on the basis of an assumed uncertainty of ±0.001 in the g values.

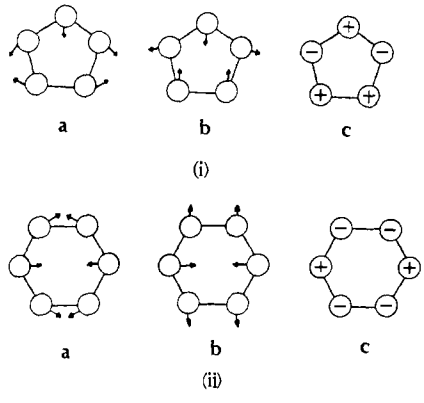

Figure 7. Jahn–Teller-active modes of e_{2g} symmetry for (i) cyclopentadiene and (ii) benzene ring distortions: (a) in-plane C–C stretch; (b) in-plane C–C–C bending; (c) out-of-plane torsion. The known experimental frequencies for typical sandwich compounds for the above three modes are as follows: 1356, 897, and 597 cm^{-1} for $Fe(Cp)_2$ (Bodenheimer, J. S.; Low, W. *Spectrochim. Acta, Part A* **1973**, *29 A*, 1733–1743) and 1630, 600, and 410 cm^{-1} for $Cr(Bz)_2$ (Cyvin, S. J.; Brunvoll, J.; Schäfer, L. *J. Chem. Phys.* **1971**, *54*, 1517–1522).

Jahn–Teller coupling strength of an active vibration is expressed as a coupling constant k_{JT} by defining k_{JT}^2 as the ratio of twice the Jahn–Teller stabilization energy to the frequency of the active vibrational mode.[21] Simple calculations of the extended Hückel type performed by making finite distortions of the molecule along the active symmetry coordinates predict a ratio of 0.35:0.63:1 for k_{JT} for the three modes in bis(benzene)iron(I). The corresponding ratio for cobaltocene is 0.79:0.35:1.[35] If one assumes a single-mode coupling involving the torsional mode and also that the distortions of the two individual rings in the case of the mixed sandwich molecules are additive, it is possible to evaluate V and tan α for various values of δ and k_{JT} by a complete diagonalization of the vibronic Hamiltonian. The procedure, described in detail in an earlier paper,[15] involves setting up and diagonalizing the matrix of the Hamiltonian in eq 1 within a $|j{:}nm\rangle$ basis, where the quantum number $j = \pm 1$ denotes the electronic orbital angular momentum around the symmetry axis, $n = 1, 2, \ldots, \infty$ is the vibrational quantum number for the two-dimensional harmonic oscillator,[36] and $m = n - 1, n - 3, \ldots, -n + 1$ is the nuclear pseudoangular momentum quantum number.[37] The vibronic

(35) Zoller, L.; Lüthi, H. P.; Ammeter, J. H., unpublished results.

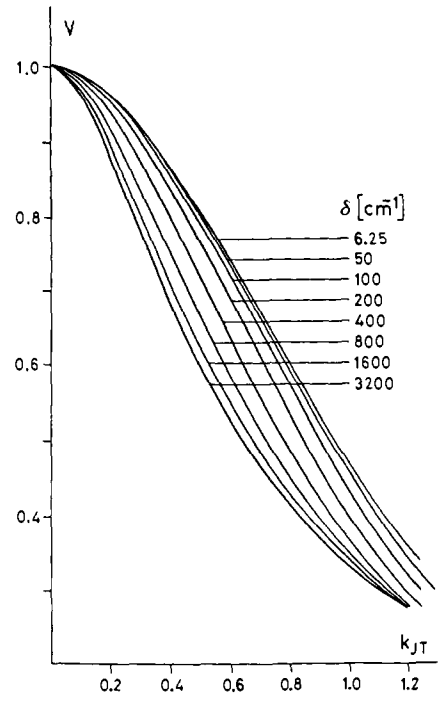

Figure 8. Vibrational overlap integral, V, for the ground vibronic state as a function of the Jahn–Teller coupling constant, k_{JT}, for various values of the rhombic distortion, δ, based on a complete diagonalization of the vibronic Hamiltonian (for $k_{\parallel} = 0.85$, $\zeta = 330$ cm^{-1}, $h\nu = 678$ cm^{-1}, N (basis dimension) = 30).

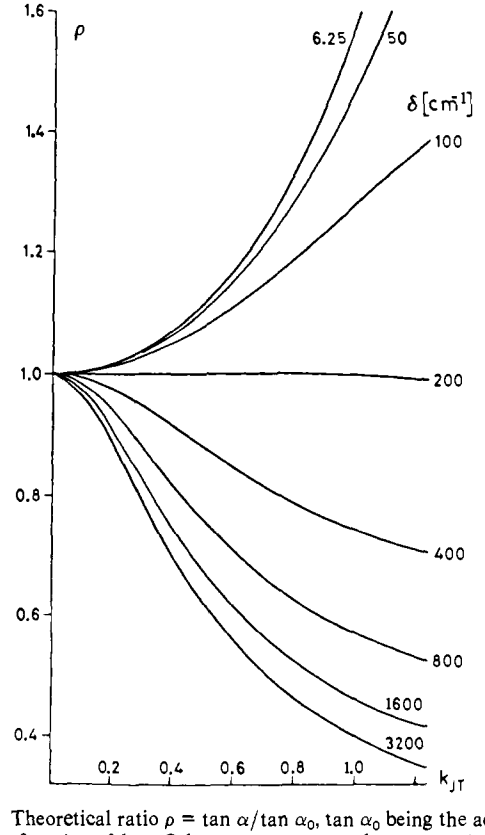

Figure 9. Theoretical ratio $\rho = \tan \alpha / \tan \alpha_0$, $\tan \alpha_0$ being the adiabatic value, as a function of k_{JT}. Other parameters are the same as for Figure 8.

(36) Pauling, L.; Wilson, E. B. "Introduction to Quantum Mechanics"; McGraw-Hill: New York, 1935.

overlap integral V for the ground vibronic state and tan α can be calculated from the resulting eigenvectors. Figure 8 shows the variation of V as a function of k_{JT} for various initial values of δ. Figure 9 is a similar plot for the ratio tan α/tan α_0, where tan $\alpha_0 = 2\delta_0/\zeta$ is the adiabatic value. The calculations were made[38] for a basis dimension of 30 (n up to 5) and with a value of 330 cm^{-1} for the spin–orbit coupling constant and 678 cm^{-1} for the vibrational frequency.[39] These plots were used for estimating graphically by an iterative process the magnitudes of k_{JT} and δ, starting with the values of V and δ_0 obtained from the **g** tensor analysis. A plot of k_{JT} vs. δ is included as an inset in Figure 6. Unlike in the case of the d^7 metallocenes[2] $Co(Cp)_2$ and $Ni(Cp)_2^+$, no smooth variation is observed in the case of Fe(I) sandwiches. We interpret this result to mean that in the present systems, the host lattice potentials have dissimilar shape in the vicinity of the Jahn–Teller minimum (see ref 4a, Figures 12–14). Since the host lattice potential felt by the dopant molecule depends on several factors, including the molecular packing in the host crystal and the minimum-energy conformation taken up by the guest molecule, smooth variation should be considered as the exception rather than the rule. It is hoped that a better understanding will be possible when explicit calculations of the host lattice perturbation of the type described in ref 4a are carried out for individual cases.

It is worth pointing out that the value of X in Table I, which is inversely related to the average energy of the excited doublet states, is fairly constant for the mixed sandwiches. There is a marked increase in its value in the case of the bis(hexamethylbenzene) compound. This is also expected because the e_{1g} orbitals are expected to be less antibonding in a bis(benzene) sandwich compared to metallocene or a mixed sandwich compound. Including the results for $Ni(Cp)_2^+$ and $Co(Cp)_2$,[2] one gets the following series for the parameter X: $Fe(hmBz)_2$ (0.012–0.013) > Fe(Cp,Bz) (0.009–0.010) ~ $Co(Cp)_2$ (0.009–0.011) > $Ni(Cp)_2^+$ (0.0064–0.0073). If one takes into consideration the small variation of the effective spin–orbit coupling constant ($\zeta \sim 300$ cm^{-1} for Fe(I) sandwiches, ~330 cm^{-1} for $Co(Cp)_2$ and $Ni(Cp)_2^+$[2]), this would mean that the energies of the first spin-allowed d–d transitions are in the following order: $Fe(hmBz)_2$ < Fe(Cp,Bz) < $Co(Cp)_2$ < $Ni(Cp)_2^+$. The shoulders or maxima at 15.15×10^3 (ϵ 17), 16.39×10^3 (ϵ 72), 17.80×10^3 (ϵ 162), and 21.19×10^3 cm^{-1} (ϵ 300) in the broad band at (15–21) $\times$ 10^3 cm^{-1} observed in the case of $Co(Cp)_2$ have been assigned to the various spin-allowed d–d transitions.[40,41] In the case of the mixed sandwich compounds a broad unresolved band is observed at (13–15 $\times$ 10^3 cm^{-1} (ϵ ~100).[6,42] On the basis of the shifts experienced on ring alkylation, we assigned this band as arising from "forbidden" M → L charge-transfer transitions. The d–d transitions are probably masked by this broad band. Bands at 17.2×10^3 (ϵ 604) and 20.9×10^3 cm^{-1} (ϵ 416) were observed in the case of $Fe(hmBz)_2PF_6$,[7] which were assigned to the spin-allowed d–d transitions.[8a] In light of the present discussion and also on the basis of the rather large extinction coefficients for these bands, we tend to favor a charge-transfer (L → M or M → L) assignment for this case also. As expected, the highest energy transitions are observed in the case of nickelocenium cation.[43] The broad band observed at (25–29) $\times$ 10^3 cm^{-1} (ϵ 562) in all probability includes charge-transfer as well as d–d transitions.

Turning now to the line width analysis, it is noteworthy that in all the cases the coefficient B turned out to be in the range 10^{-1}–10^{-2}, which is about 4 orders of magnitude smaller than the typical values observed for the Orbach process, for example, in lanthanide ions. This indicates a rather weak coupling of the spin system with the phonons of the "lattice". The small values of ΔE are incompatible with the Ham equation (eq 6), since even in the limit of infinite Jahn–Teller coupling ($p = 0$, $q = {}^1/_2$) ΔE can never become smaller than δ. This, as well as the fact that no temperature dependence of the g values was observed, leads us to suspect either that the ΔE obtained by this procedure represents some other low-energy process like ring rotation rather than the transition between the two lowest Kramers' doublets or that there are other temperature-dependent contributions to the line width (for example, the Raman process being proportional to T^7), leading to an underestimation of our Orbach ΔE. Considering the NMR[44] and ENDOR[33] evidence for the temperature dependence of the ring rotation frequency in metallocenes exceeding the EPR time scale only at relatively high temperatures, we favor the latter alternative.

Conclusions

(1) Iron(I) sandwich complexes diluted in several diamagnetic host systems have been investigated by EPR at low temperatures. The g values lie between 2.01 and 1.30 and depend on the host lattice. In agreement with the expectation for a d^7 ($^2\pi$) ground state, g_z is always less than the free electron value.

(2) The spectra reported earlier by Nesmeyanov et al.,[5] with $g_\parallel = 2.07$–2.25 and $g_\perp = 2.006$, also attributed to Fe(I) sandwich compounds, must originate from another species. These spectra are similar to those of highly distorted ferrocenium salts[14c] and possibly originate from decomposition products containing Fe(III) d^5.

(3) From our results there is no evidence for a low-lying excited state with the unpaired electron located in a ligand level corresponding to an Fe(II) d^6 complex with a radical anion ligand ring. Such an alternative had been proposed by Clack and Warren[10] for the ground state of Fe(Cp,Bz) on the basis of INDO-type semiempirical MO calculations. In fact the optical absorption spectra indicate that this level is located at least 13×10^3 cm^{-1} above the d^7 ground level.

(4) As in the case of d^7 Co(II) and Ni(III) metallocenes,[2,4] there is clear evidence for dynamic Jahn–Teller motion in the ground Kramers' doublet from the low orbital angular momentum reduction factor of 0.2–0.5, from the characteristic host lattice dependence of the g values, and also from the characteristic temperature variation of the EPR line width. As in the case of d^7 metallocenes, the Jahn–Teller coupling parameter k_{JT}^2 is of the order of unity. While the EPR data do not allow a determination of the exact nature of the active vibronic coupling mode, extended Hückel MO calculations indicate that the dominant contribution comes from the out-of-plane e_{2g} ring distortion modes for Cp and benzene rings.

(5) As in the case of $Co(Cp)_2$ and $Ni(Cp)_2^+$, the Jahn–Teller coupling parameter, k_{JT}, on the average, decreases somewhat with increasing asymmetric host lattice potential δ, but there is significantly more scatter than in the metallocene cases. This indicates that the various host lattice potentials acting upon the iron(I) guest molecules along the active modes have different curvatures from host to host.[4a]

(6) The temperature dependence of the EPR line width could be fitted to the Orbach model.[27] Consistent with the predictions of the harmonic first-order vibronic coupling model of Longuet-Higgins et al.[37a] modified for low symmetry and spin–orbit coupling by Ammeter and Swalen,[15] the most axial host lattices give the smallest ΔE, but the surprisingly small values of ΔE indicate that contributions from other relaxation processes (e.g., Raman) cannot be ruled out. The Orbach ΔE values of Table II therefore seem to represent a lower limit, while the higher

(37) (a) Longuet-Higgins, H. C.; Opic, V.; Pryce, M. H. L.; Sack, R. A. *Proc. R. Soc. London, Ser. A* **1958**, *A244*, 1–16. (b) McConnell, H. M.; McLachlan, A. D. *J. Chem. Phys.* **1961**, *34*, 1–12.

(38) Oswald, N. Thesis, Swiss Federal Institute of Technology, 1977. The restricted vibrational basis set employed was sufficient to give convergence for the lowest vibronic levels only.

(39) These values apply to cobaltocene. Both these numbers are expected to be smaller for iron(I) bis(benzene) or mixed sandwich compounds. In the present case this will lead to a small overestimate of k_{JT} and an underestimate of δ but will not greatly affect the appearance of the k_{JT}–δ plot.

(40) Gordon, K. G.; Warren, K. D. *Inorg. Chem.* **1978**, *17*, 987–994.

(41) Weber, J.; Goursot, A.; Pénigault, E.; Ammeter, J. H.; Bachmann, J., submitted for publication.

(42) Hamon, J.-R.; Astruc, D.; Rajasekharan, M. V.; Ammeter, J. H.; Giezynski, S. "Proceedings of the Twenty-First International Conference on Coordination Chemistry"; Toulouse, 1980; p 357.

(43) (a) Borrel, P.; Henderson, E. *Inorg. Chim. Acta* **1975**, *12*, 215–218. (b) Bachmann, J.; Ammeter, J. H., unpublished results.

(44) Holm, C. H.; Ibers, J. A. *J. Chem. Phys.* **1959**, *30*, 885–888.

estimate from the Ham relation (eq 6) rests on the assumption of an effective frequency of the Jahn–Teller coupling mode of $\sim$700 cm^{-1}. Electronic Raman or inelastic neutron scattering experiments seem to be necessary for an unambiguous location of the excited Kramers' doublet, thereby allowing a determination of the effective frequency.

(7) The average energies of the spin-allowed d–d transitions estimated for several d^7 metallocenes, mixed sandwiches, and bis(benzene) compounds are within an order of magnitude agreement with experimental values. Further, the **g** tensor analysis predicts the correct sequence for the energies of these transitions for the various d^7 sandwich compounds.

(8) The observation of four chemically inequivalent sites for Fe(Cp,Bz) in $Fe(Cp)_2$ is in agreement with the expectation from the low-temperature crystal structure of triclinic ferrocene.[31]

Acknowledgment. We thank Professor François Varret and Jean-Pierre Mariot from the University of Le Mans for stimulating discussions. We thank M. Heinzle for secretarial assistance. This work has been supported by the Swiss National Science Foundation (Project No. 2.683-0-80).

Registry No. Fe(Cp,Bz), 51812-05-6; Fe(Cp,hmBz), 70414-92-5; Fe(hmBz)$_2$PF$_6$, 53382-61-9; Fe(pmCp,hmBz), 71713-53-6; Fe(Cp,heBz), 71713-55-8; Fe(Cp,(pm,e)Bz), 71742-81-9.

Coordination Behavior of L-Aspartic Acid: Ternary Nickel(II) Complexes with Imidazoles. Crystal and Molecular Structure of (L-Aspartate)tris(imidazole)nickel(II)

L. P. Battaglia,[1a] A. Bonamartini Corradi,[1a] L. Antolini,[1b] G. Marcotrigiano,[1c] L. Menabue,[1b] and G. C. Pellacani*[1b]

Contribution from the Consiglio Nazionale delle Ricerche, Rome, Italy, Istituto di Chimica Generale, Centro di Studio per la Strutturistica Diffrattometrica del C.N.R., University of Parma, Parma, Italy, the Istituto di Chimica Generale ed Inorganica, University of Modena, Modena, Italy, and the Istituto di Chimica, Facoltà di Medicina-Veterinaria, University of Bari, Bari, Italy. *Received July 13, 1981*

Abstract: Two ternary compounds of formula Ni(L-asp)B_3 (L-asp = L-aspartate ion; B = imidazole and 2-methylimidazole) were prepared and characterized by means of magnetic and spectroscopic measurements. For one of them, the Ni(L-asp)$(im)_3$ complex, the crystal structure was also determined. The compound crystallizes in the monoclinic space group $P2_1$ with four formula units in a cell of dimensions a = 22.001 (2) Å, b = 8.631 (1) Å, c = 8.514 (1) Å, and β = 95.07 (1)°. X-ray diffraction data were collected with a Philips PW 1100 automated four-circle diffractometer by using Mo Kα radiation. The structure was solved by the heavy-atom method and refined by full-matrix least-squares procedures to a final R factor of 0.0514 for 2051 independent reflections. The structure consists of two crystallographically independent but chemically equivalent Ni(L-asp)$(im)_3$ molecules in which each Ni atom is coordinated in a distorted octahedral geometry by one L-aspartate ion, acting as a tridentate ligand, and by three imidazole molecules. Infrared and ligand field spectroscopies and magnetic measurements all agree with the observed crystal structure.

There is great interest in the coordination ability of aspartic acid to metal ions, from either a biological or simple coordinative point of view. The majority of reports are based on solution studies, in which it was generally suggested that aspartate usually acts as a tridentate ligand,[2] while the few structural results, performed on solid compounds, show changeable behavior depending on the metal ion to which the amino acid is coordinated. In fact, the aspartate ion acts as truly tridentate to the same metal ion only in bis(L-aspartate)cobalt(III) complexes,[3] being tetradentate bridging two zinc(II) ions or three copper(II) ions in zinc(II) aspartate trihydrate[4] or in (L-aspartate)(imidazole)copper(II) dihydrate,[5] respectively.

Our interest in the solid-state complexes of aspartic acid began with a study of its ternary copper(II) complexes with amines[5] in the attempt to rationalize its different coordination behavior and is now extended to the investigation of the spectroscopic, magnetic, and structural properties of two mixed-ligand complexes of the nickel(II) with L-aspartic acid and imidazole or 2-methylimidazole (L-aspH, im, and 2Meim, respectively).

The presence of small biologically important molecules in these complexes, which makes them usable as models for more complicated systems, and the presence of heteroatomic N base moieties and O donors in the coordinative sphere of the nickel(II) ion, a combination of donor atoms present in many naturally occurring mixed-ligand complexes and recognized as enhancing the complex stability,[6] also confer some interest on this work from the biological point of view.

Experimental Section

Preparation of (L-Aspartate)tris(imidazole)nickel(II) Complex, Ni(L-Asp)$(im)_3$. By dissolving a mixture of Ni(L-asp)·$3H_2O$ (1 mmol) and imidazole (2 mmol) in boiling water and slowly evaporating the solution at 20 °C, we separated blue violet crystals. Anal. Calcd for

(1) (a) University of Parma. (b) University of Modena. (c) University of Bari.

(2) Evans, A. G.; Guevremont, R.; Rabenstein, L. D. In "Metal Ions in Biological Systems"; Sigel, H., Ed.; Marcel Dekker: New York, 1979; Vol. 9, p 41 and references cited therein.

(3) Oonishi, I.; Sato, S.; Saito, Y. *Acta Crystallogr., Sect. B* **1975**, *B31*, 1318.

(4) (a) Doyne, T.; Pepinsky, R.; Watanabe, T. *Acta Crystallogr.* **1957**, *10*, 438. (b) Kryger, L.; Rasmussen, S. E. *Acta Chem. Scand.* **1973**, *27*, 2674.

(5) Antolini, L.; Marcotrigiano, G.; Menabue, L.; Pellacani, G. C.; Saladini, M., *Inorg. Chem.*, in press.

(6) Sigel, H. *Inorg. Chem.* **1980**, *19*, 1411 and references cited therein.

0002-7863/82/1504-2407$01.25/0